ARTICLE
Journal of Cellular Biochemistry 113:302–312 (2012)

Journal of Cellular Biochemistry

Identification of Cancer Stem Cells in Vincristine Preconditioned SGC7901 Gastric Cancer Cell Line

Zengfu Xue,[1,2] Hui Yan,[1] Juntang Li,[3] Shuli Liang,[1] Xiqiang Cai,[1] Xiong Chen,[1] Qiong Wu,[1] Liucun Gao,[1] Kaichun Wu,[1] Yongzhan Nie,[1*] and Daiming Fan[1*]

[1] *State Key Laboratory of Cancer Biology & Institute of Digestive Diseases, Xijing Hospital of Digestive Diseases, Xi'an 710032, China*

[2] *Department of Digestive Diseases, The First Affiliated Hospital of Xiamen University, 10 Shanggu Road, Xiamen 361003, China*

[3] *Department of Immunology, the Fourth Military Medical University, 17 Changle Western Road, Xi'an 710032, China*

ABSTRACT

Cancer stem cells (CSCs), or tumor initiating cells, are a subpopulation of cancer cells with self-renewal and differentiation properties. However, there has been no direct observation of the properties of gastric CSCs in vitro. Here we describe a vincristine (VCR)-preconditioning approach to obtain cancer stem-like cells (CSLCs) from the gastric cancer cell line SGC7901. The CSLCs displayed mesenchymal characteristics, including the up-regulated mesenchymal markers Snail, Twist, and vimentin, and the down-regulated epithelial marker E-cadherin. Using a Matrigel-based differentiation assay, CSLCs formed 2D tube-like and 3D complex lumen-like structures, which resembled differentiated gastric crypts. The characteristic of cellular differentiation was also found by transmission electron microscopy and up-regulation of gastrointestinal genes CDX2 and SOX2. We further showed that CSLCs could self-renew through significant asymmetric division compared with parent cells by tracing PKH-26, BrdU, and EDU label-retaining cells. In addition, these CSLCs also increased expression of CD44, CD90, and CXCR4 at the mRNA level, which was identified as novel targets. Furthermore, drug sensitivity assays and xenograft experiments demonstrated that the cells developed multi-drug resistance (MDR) and significant tumorigenicity in vivo. In summary, gastric CSCs were identified from VCR-preconditioned SGC7901 cell line, characterized by high tumorigenicity and the capacity for self-renewal and differentiation. J. Cell. Biochem. 113: 302–312, 2012.

KEY WORDS: GASTRIC CANCER; DIFFERENTIATION; SELF-RENEWAL; CANCER STEM CELLS; VINCRISTINE

The study of cancer stem cells (CSCs), especially in solid tumors, has deeply influenced our understanding of carcinogenesis and chemotherapy [Dean et al., 2005]. Cancer often exhibits heterogeneity in its proliferative and invasive capacities [Rosen and Jordan, 2009]. CSCs and their clonal evolution models have explained the heterogeneity and inherent differences in tumors [Visvader and Lindeman, 2008; Rosen and Jordan, 2009]. CSCs are a population of cells that retains the ability to self-renew while possessing the ability to differentiate into progeny [Eyler and Rich, 2008]. CSCs also share other normal stem cell characteristics, such as resistance to drugs and relative quiescence [Bjerkvig et al., 2005; Gupta et al., 2009a]. The evidence that indicates the existence of CSCs first came from acute myeloid leukemia and then from solid cancers, such as breast, colon, and lung cancers [Morel et al., 2008; Visvader and Lindeman, 2008; Todaro et al., 2010].

Gastric cancer remains one of the most common cancers and a leading cause of mortality in the world, despite the recent decrease in its incidence [Parkin et al., 2005]. It is therefore important to quickly and accurately identify gastric CSCs for targeted treatment. Several groups have identified different gastric epithelial progenitor

Disclosure of potential conflicts of interest: The authors indicate no potential conflicts of interest.

Zengfu Xue and Hui Yan contributed equally to this work.

Additional Supporting Information may be found in the online version of this article.

Grant sponsor: National Basic Research Program of China; Grant numbers: 2010CB529300, 2010CB529306 and 2010CB529302; Grant sponsor: National Natural Science Foundation of China; Grant number: 30871143 and 3087114.

*Correspondence to: Yongzhan Nie and Daiming Fan, State Key Laboratory of Cancer Biology & Institute of Digestive Diseases, Xijing Hospital of Digestive Diseases, the Fourth Military Medical University, 17 Changle Western Road, Xi'an 710032, China. E-mail: nieyong.zhan@gmail.com, daimingfan@fmmu.edu.cn

Received 1 September 2011; Accepted 6 September 2011 • DOI 10.1002/jcb.23356 • © 2011 Wiley Periodicals, Inc.
Published online 12 September 2011 in Wiley Online Library (wileyonlinelibrary.com).

markers [Qiao et al., 2007; Barker et al., 2010]. For example, villin-positive cells from the gastric antrum gave rise to all of the different lineages of a gland in Villin-Cre mice using the lineage tracing method [Qiao et al., 2007].

Recently, Lgr5 gastric stem cells were shown to have self-renewal and differentiation properties in vitro and in vivo [Barker et al., 2010]. It was first proven that single Lgr5(+ve) stem cells could efficiently generate gastric organoids, which resembled the gastric pyloric gland, in vitro. However, there was no significant difference in the expression of Lgr5 between CD44-positive gastric CSCs and CD44-negative cells [Takaishi et al., 2009]. Therefore, Lgr5 might not be suitable for the study of gastric CSCs. CD44-positive gastric CSCs were also able to give rise to glandular cells upon transplantation into the stomachs of SCID mice [Takaishi et al., 2009]. However, some gastric cancer cell lines can contain high proportions of CD44-positive cancer cells, this is not consistent with the current CSCs models [Dean et al., 2005]. And, there is still a lack of knowledge about the homeostasis of gastric CSCs, especially in differentiation and self-renewal, which hampers the study of gastric stem cells and CSCs [Barker et al., 2010].

The epithelial–mesenchymal transition (EMT) facilitates cancer metastasis and survival by transdifferentiation, in which a tumor loses epithelial characteristics and acquires a mesenchymal phenotype [Kalluri and Weinberg, 2009]. This phenotype transition enriches the subpopulation of CSCs, which have proven tumor seeding, sphere formation, and invasive properties [Ansieau et al., 2008; Mani et al., 2008; Morel et al., 2008; Gupta et al., 2009a]. Some types of chemotherapeutics, such as adriamycin (ADR), gemcitabine, 5-fluorouracil, and cisplatin, induce the EMT in breast and pancreatic cancers [Arumugam et al., 2009; Wang et al., 2009; Li et al., 2009]. Unfortunately, this drug-induced mesenchymal phenotype change enhances multi-drug resistance (MDR) and invasiveness in vitro. High-throughput experimental methods have thus been adopted to screen for drugs that kill the rare epithelial CSCs enriched by EMT [Gupta et al., 2009b]. The advantages of obtaining CSCs by inducing the EMT are the easy enrichment of CSCs and the relative stability in culture of these cell lines [Gupta et al., 2009b; Yeung et al., 2010]. Because CSCs are generally only small populations within cancer cells, standard high-throughput screening cannot be applied to identify drugs with CSC-specific toxicity in vivo. Furthermore, searching for agents that effectively kill CSCs depends on propagation stability in vitro [Gupta et al., 2009b]. Hence, identifying and developing new methods to induce the EMT for enriching CSCs is one of the better choices for the study of CSC target therapy.

For a decade, vincristine (VCR) and ADR drug-resistant cell lines have been established and applied to the study of mechanisms of MDR in our laboratory [Xia et al., 2008; Zhao et al., 2009]. We have found that the up-regulation of mesenchymal markers, such as Twist, Snail, and vimentin, in these cell lines is correlated with the concentration of drug. To investigate whether chemotherapeutics can induce gastric cancers to dedifferentiate into gastric CSCs or cancer stem-like cells (CSLCs), we established a novel model of inducing CSLCs by VCR in ultra-low-attachment culture medium. Then, we demonstrated that CSLCs up-regulated the stem cell markers and high tumorigenicity in vivo. We further showed that VCR-induced CSLCs were able to self-renew and differentiate. In addition, the induced gastric CSCs had enhanced chemoresistance. Finally, surface markers were screened by real-time PCR, which will benefit the screening of gastric CSCs in future studies.

MATERIALS AND METHODS

CANCER CELL LINES

The poorly differentiated human gastric adenocarcinoma cell line SGC7901 was obtained from the Academy of Military Medical Science (Beijing, China). MKN28 and AGS cell lines were purchased from ATCC (Rockville, MD). Cells were maintained in RPMI-1640 medium containing 10% heat-inactivated fetal calf serum (GIBCO, Carlsbad, CA) at 37°C and 5% CO_2. Cells were observed by light (Olympus BX51, Olympus, Tokyo, Japan) and transmission electron microscopy (JEM-2000EX, JEOL, Tokyo, Japan).

SPHEROID COLONY FORMATION ASSAY

SGC7901 cells were treated with VCR (1 μg/ml) for 3 days (VCR-induced cancer cells). The surviving cells were inoculated in the wells (200 cells per well) of ultra-low-attachment 96-well plates (Corning Life Sciences, Acton, MA, www.corning.com). The CSC medium was supplemented with DMEM/F12 (Invitrogen), human recombinant epidermal growth factor (EGF, 20 ng/ml, Invitrogen, http://www.invitrogen.com) and human recombinant basic fibroblast growth factor (bFGF, 20 ng/ml, Invitrogen). Cell viability was examined by trypan blue (Sigma–Aldrich) at different time points. After 5 weeks, dead cells were removed by centrifugation, and the remaining cells were expanded to 24- or 6-well plates. AGS and MKN28 tumor sphere studies followed the above methods.

PLATE CLONE FORMATION ASSAYS

CSLCs and SGC7901 cells seeded at 1,000 cells in each 6-well plate and cultured in RPMI-1640 medium containing 10% heat-inactivated fetal bovine serum (FBS) for about 14 days. When most cell clones reached more than 50 cells, fixed with 4% paraformaldehyde for 15 min, and stained with 1% crystal violet at room temperature. Each experiment repeated three times.

DIFFERENTIATION ASSAYS

For 2D differentiation assays, single-cell suspensions were placed on Matrigel-coated plates at a density of 500 viable cells/well in 96-well plate. Cells were grown in DMEM/F12 with 10% FBS and 10 ng/ml of EGF. After 7 days, vessel-like structures were observed by light microscopy. A layer of Matrigel was added to each well of a 24-well glass chamber slide for 3-D culture. While the Matrigel solidified, cells (200 viable cells/well) were mixed with 2% Matrigel and 10 ng/ml EGF and seeded on the plate [Debnath et al., 2003; Dontu et al., 2003; Pece et al., 2010]. Complex, lumen-like colonies were clearly observed by microscope 7 days later. The structures were also observed by immunofluorescence when the nucleus was stained with DAPI.

SELF-RENEWAL ASSAY

PKH-26 staining. Cells were re-suspended in CSC medium (200,000 cells/ml) and labeled with PKH26 (MINI26, 10^{-7} M, 5 min, Sigma, St. Louis, http://www.sigmaaldrich.com) [Cicalese et al., 2009]. Briefly, tumor spheres were harvested, dissociated, and counted. PKH26 dye was diluted with the dilution mediate and mixed with cells for 5 min according to manufacturer's instructions. A twofold dilution of FBS was added to stop the staining process. After washing 3 times with CSC medium, labeled cells were plated (1,000 cells/ml) in 96-well ultra-low-attachment plates for fluorescent microscope examination. Cell viability was observed under light microscopy or by staining with trypan blue.

BrdU and EDU labeling assay. The BrdU methods modified from Pine et al. [2010] methods. Briefly, BrdU (Sigma–Aldrich) was added to the culture medium at a concentration of 2 μM for 1 weeks to ensure the labeling cells growing for up to 3–4 passages. The BrdU medium was supplemented with every 72 h, and keep cell growth in log phase. Edu was add 25 μM/ml for 24 h to chase the template of DNA and followed the manual (C00031, Apollo 567, RiboBio, China). Briefly, after fixed in 4% paraformaldehyde and treated with 0.5% Triton-X for 15 min, cells were incubated in with Apollo, and staining nucleus by Hoechst 33342.

WESTERN BLOT ANALYSIS

Cells were washed twice with PBS and lysed directly in radioimmunoprecipitation assay buffer (50 mM Tris–HCl [pH 7.4], 1% [v/v] Triton X-100, 1 mM EDTA, 1 mM phenylmethylsulfonyl fluoride, 10 mM NaF, and 1 mM Na_3VO_4). The lysates were centrifuged at 12,000 rpm for 10 min at 4°C, and the supernatants were collected. Thirty micrograms of protein was loaded onto an 8% SDS–PAGE gel, subjected to electrophoresis at 20 mA for 80 min under denaturing conditions and then transferred to nitrocellulose. The membrane was blocked with 5% non-fat dry milk in PBS for 2 h and then probed with primary antibodies to vimentin (A2547) (1:1,000, Sigma–Aldrich) and E-cadherin (G-10) (1:100, Santa Cruz, CA, www.scbt.com). After repeated washing, the membranes were incubated with horseradish peroxidase-conjugated anti-rabbit or anti-mouse secondary antibody (Ab) (Sigma–Aldrich) diluted 1:5,000. The bands were then detected by an enhanced chemiluminescence (ECL) system (Amersham Pharmacia Biotech, Arlington Heights, www.gelifesciences.com).

IMMUNOFLUORESCENCE STAINING

The CSLCs and parental cell line SGC-7901 were plated for 4 h on sterilized coverslips in 24-well plates. The cells were fixed in 4% paraformaldehyde (room temperature, 10 min), washed with PBS, treated with 0.25% Triton-X for 15 min, blocked with 10% goat serum for 30 min, incubated with primary antibodies overnight and thawed for 1 h at room temperature (RT). Cells were immunostained for Oct4 (1:200), OCT-4A (1:800), and SOX2 (1:400) (all from Cell Signaling, USA, www.cellsignal.com). The secondary antibody (1:400) used was donkey anti-mouse IgG-Cy3 (Molecular Probes, Invitrogen, www.invitrogen.com). The cells were counterstained with the nuclear dye DAPI (Sigma) and examined with a fluorescence microscope. Differentiated cells stained with DAPI were examined by a FluoView FV1000 laser scanning confocal microscope (Olympus). Analysis of 3D reconstructions was done by using FV10-ASW Viewer 2.0 software.

The methods for BrdU. Briefly, cells were fixed in 4% paraformaldehyde, and incubated in 2 N HCl containing 0.5% Triton-X-100 for 1 h [Pine et al., 2010]. Cells were washed with PBS, blocked with 10% goat serum for 30 min, and incubated with a 1:100 dilution of mouse anti-BrdU (BM0201, Boster, China) and the secondary antibody (1:400, donkey anti-mouse IgG-FITC, Molecular Probes) follow the above-mentioned methods.

REAL-TIME PCR (RT-PCR)

Total RNA was isolated using the TRIzol reagent according to the manufacturer's instructions (Invitrogen). Reverse transcription (RT) reactions were performed using 2 mg of total cellular RNA with a PrimeScript RT reagent kit and SYBR premix Ex Taq (Takara, China, www.takara.com.cn) to detect the target genes. RT-PCR amplification was performed as follows: initial denaturation for 2 min at 95°C followed by 45 cycles of PCR (95°C for 15 s, 58°C for 20 s, and 72°C for 15 s). GAPDH was adopted as the housekeeping gene. The fold changes for each mRNA were calculated using the $2^{-\Delta\Delta CT}$ method. The different forward (F) and reverse (R) primer sequences are shown in Table I.

IN VITRO DRUG SENSITIVITY ASSAY

VCR, epirubicin (EPI), ADR, and 5-fluorouracil (5-FU) were assessed in this experiment. The sensitivity of VCR-induced cancer cells and

TABLE I. The Primers Used for Real-Time PCR for Stem Cells and EMT Markers

Gene names	5′–3′
OCT-4	
Forward	CCTGAAGCAGAAGAGGATC
Reverse	CGTTTGGCTGAATACCTT
SOX2	
Forward	CCAGCTCGCAGACCTACAT
Reverse	ACTTGACCACCGAACCCA
Bmi-1	
Forward	TGACTCTGGGAGTGACAAGG
Reverse	TGTGAGGAAACTGTGGATG
EpCam	
Forward	ATCGTCAATGCCAGTGTAC
Reverse	CTGCCTTCATCACCAAAC
GAPDH	
Forward	GCACCGTCAAGGCTGAGAAC
Reverse	TGGTGAAGACGCCAGTGGA
CXCR4	
Forward	AATGGGCTCAGGGGACTA
Reverse	GATGGTGGGCAGGAAGAT
Musashi-1	
Forward	ACGCCATGCTGATGTTTG
Reverse	TCCACGATGTCCTCACTCT
CD90	
Forward	ACCCGTGAGACAAAGAAGC
Reverse	GGCGGATAAGTAGAGGACC
CD133	
Forward	TACGGCACTCTTCACCTG
Reverse	TCACTGCTTATGCTTCCAG
CD44	
Forward	CAAGCAATAGGAATGATGTC
Reverse	GGTCACTGGGATGAAGGT
Snail	
Forward	CCAGTGCCTCGACCACTATG
Reverse	GCAGCTCGCTGTAGTTAGGCTTC
Twist	
Forward	GGCCAGGTACATCGACTTCC
Reverse	CCGCTCGTGAGCCACATA

SGC7901 cells was evaluated using 3-(4,5-dimethylthiazol-2-yl)-2, 5-diphenyl-tetrazolium bromide (MTT) assay. Cells were incubated for 72 h in the presence of various concentrations of the anticancer agents, and the IC_{50} values (the concentration of each drug produced 50% inhibition of tumor cells growth) were determined. Each experiment was repeated three times.

IN VIVO EXPERIMENTS

Four-week-old BALB/C-nu/nu nude mice (male) were obtained from the Shanghai Laboratory Animal Center of China. VCR-induced CSLCs (1×10^5) and their parental cell line SGC7901 (1×10^5 cells) were injected subcutaneously. Each group contained six mice. Mice were monitored every 3 days for tumor growth for up to 8 weeks. After 8 weeks, the mice were euthanized, and tissues from subcutaneous xenografts were histologically examined. Nude mice experiments were performed with the approval of the Institutional Committee for Animal Research and in conformity with national guidelines for the care and use in the Experiment Animal Center of the Fourth Military Medical University (2010-09-012, Xi'an, Shanxi Province, P.R. China).

FLOW CYTOMETRY

Briefly, 1.0×10^6 cells were trypsinized, washed twice with PBS and immunostained for 20 min on ice with monoclonal antibodies against CD44 (PE-conjugated) (Becton Dickinson, San Jose, CA). Labeled cells were analyzed using a flow cytometer (FACS Calibur, Becton Dickinson). Background signals were established using control cells incubated with isotype-specific IgGs.

STATISTICAL ANALYSIS

One-way ANOVA and Student's *t*-test were employed to analyze the data using SPSS 13.0 software (Chicago, IL, USA). A *P*-value <0.05 was defined as statistically significant.

RESULTS

TRANSIENT DRUG TREATMENT-INDUCED GASTRIC CANCER EMT AND TUMOR SPHERE FORMATION

The morphology of cultured SGC7901 cells treated with or without VCR and ADR for 72 h was examined microscopically. VCR-induced SGC7901 cells were found to lose cell–cell contacts and to acquire fibroblast phenotypes as a result of transient VCR treatment (Fig. 1A,B). Similar phenotypes were also observed in other gastric cancer cell lines MKN28 and AGS. We further found that Snail and Twist, which are two critical mesenchymal markers, were up-regulated at the mRNA level in treated cells (Fig. 1C). Additionally, MDR response genes, such as MRP and Pgp, were up-regulated (Fig. 1C). Because the loss of the epithelial marker E-cadherin and a corresponding increase in mesenchymal markers, including vimentin, are the hallmarks of the EMT [Zeisberg and Neilson, 2009], we assessed the protein levels of E-cadherin and vimentin in cells treated with different concentrations of VCR. As expected, a decrease in E-cadherin and up-regulation of vimentin were observed (Fig. 1D).

The ability of VCR-preconditioned cells to form spheroids (considered to be one characteristic of CSCs [Gupta et al., 2009b]) was next explored after a 3-day treatment. Tumor sphere bodies formed in significant numbers in cells with transient VCR treatment (Fig. 1E), while few SGC7901 cells formed sphere bodies without VCR treatment (Fig. 1F). VCR-preconditioned SGC7901 significantly increased rate of tumor sphere formation ($P < 0.05$, Fig. 1G). Furthermore, tumor spheroid cells were prepared into single cell suspension and seeded in 96-well plates at 1–10 cells/well in 0.2 ml serum-free medium. Significant spheroid formation was observed with the expansion of time (Fig. 1H1–H3). In addition, the MKN28 and AGS cell lines also generated significant tumor spheres similar with SGC7901 (Supplement Figure).

The viability of tumor spheroid cells at different time points was subsequently investigated with trypan blue. After 2 weeks, more than 90% of the cells had survived in serum-free media. Additionally tumor spheroid bodies did form and were viable for a long time. Few of the SGC7901 cells without treatment were found alive in the serum-free media. This striking heterogeneity of tumor sphere formation has also been reported in other cell models, including U87 glioblastoma cells and SW1222 colon cancer cells [Yu et al., 2008; Yeung et al., 2010].

GASTRIC CSLCs EXHIBITED DIFFERENTIATION ABILITY AND SELF-RENEWAL ABILITY IN VITRO

To study the differentiation of CSLCs of gastric cells, we first used transmission electron microscopy to examine the morphological changes. The small primary cells were easily identified by their lack of a nucleolus accompanied by small amounts of cytoplasm and organelles (Fig. 2B), which is consistent with stem cells [Sathananthan and Nottola, 2007]. However, more heterochromatin and organelles, such as mitochondria, were found in the parental cell line SGC7901 than in VCR-induced CSLCs (Fig. 2A). Surprisingly, gland-like structures were observed in gastric CSLCs that contained microvilli in their cavities (Fig. 2B) and comprised the luminal surface of gland cells [Fisher and Cooper, 1967]. These gland-like structures were composed of one primary cell and two differentiated cells.

Consequently, the differentiation ability of VCR-induced CSLCs was explored in a 2D Matrigel differentiation assay. Seven days after seeding on Matrigel [Yeung et al., 2010], VCR-induced CSLCs showed confluence and formed tube-like structures (Fig. 2D). In contrast, the parental SGC7901 cells failed to form tube-like structures under identical conditions (Fig. 2C).

We also used 3D Matrigel [Debnath et al., 2003; Barker et al., 2010; Yeung et al., 2010] to assess the property of gastric gland organotypic growth. Single cells were plated by limited dilution in 96-well Matrigel-containing plates. Approximately 70% of the cells differentiated into large, complex structures with gland-like formation 2 weeks later. We explored the inner structure of colonies through 3D reconstruction using laser scanning confocal microscopy by staining with DAPI. Complex lumen-like structures were embedded in them (Fig. 2E1–E3). In addition, gastrointestinal genes CDX2 and SOX2 were significantly up-regulated, explored by real-time PCR (Fig. 4B).

To identify the self-renewal property in CSLCs, we employed a lipophilic fluorescent dye, PKH-26, which stains the rare quiescent subpopulations, and examined the asymmetric and symmetric

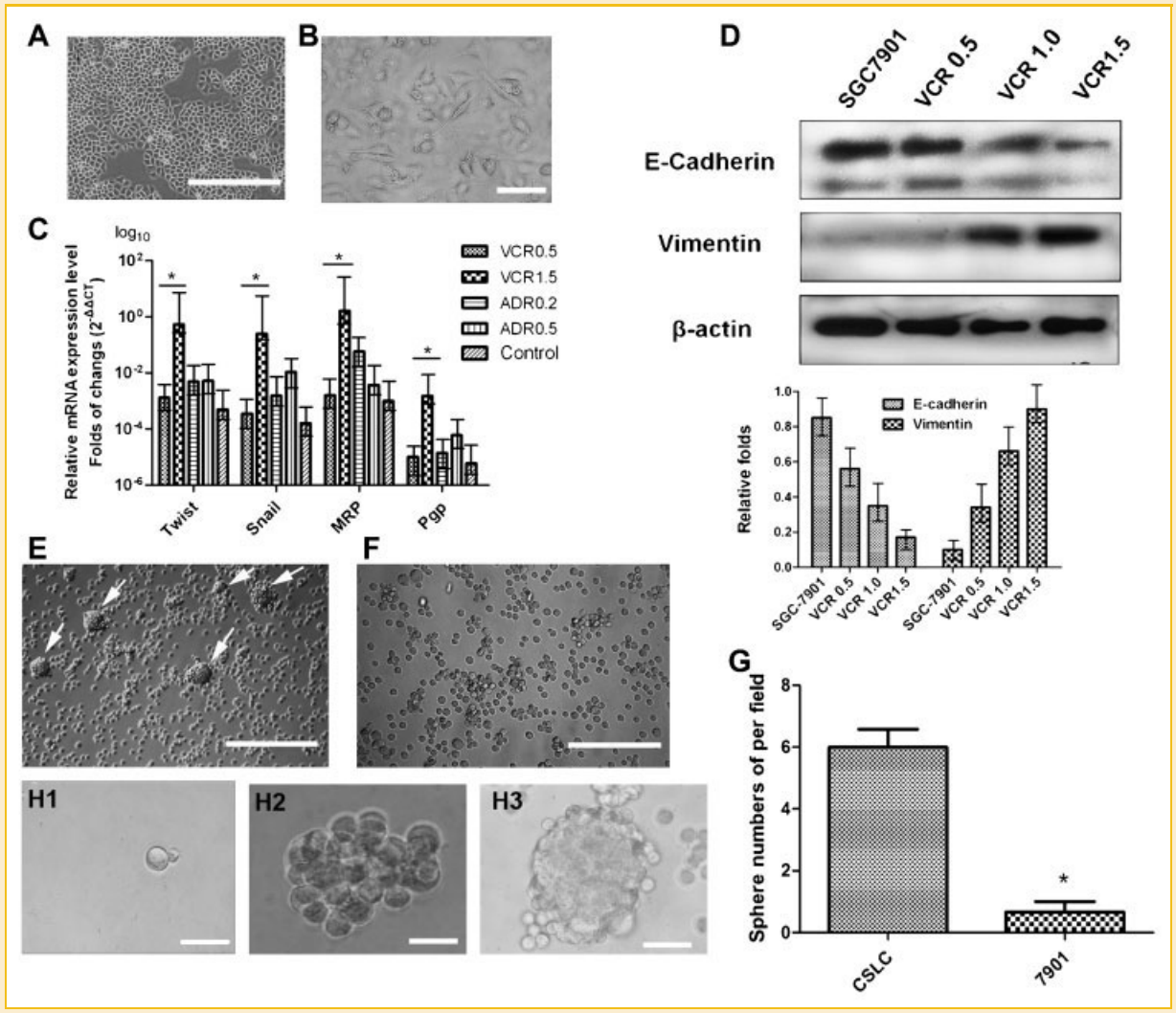

Fig. 1. VCR-preconditioning SGC7901 cells that show a mesenchymal phenotype and stem cell-like properties. A: SGC7901 cells. B: SGC-7901 cells transiently induced by VCR (1 μg/ml) with a disperse and fibroblast-like phenotype. C: The Snail, Twist, MRP, and Pgp genes were up-regulated with VCR (0.5 and 1.5 μg/ml). No difference was observed after ADR treatment (0.2 and 0.5 μg/ml). D: Up- and down-regulation of E-cadherin and vimentin were found after 0.5, 1.0, and 1.5 μg/ml VCR treatments. Moreover, quantitative analyses were performed, VCR-preconditioning SGC7901 (E) showed significant tumor spheres (arrow) but few of SGC7901 formed in serum-free condition within 2 weeks (F,G). Single cancer stem cell (H1) grows as a tumor sphere (H2, 3 weeks and H3, 6 weeks) (Scale bar, 200 μm; asterisk, $P < 0.05$, Student's *t*-test).

division to identify cancer-initiating cells by the amount of retained dye [Pece et al., 2010]. As such, dispersed sphere cells were labeled with PKH-26 and cultured in suspension to allow tumor sphere body growth. After 1 day, a few cells had symmetrically divided into two cells, and the daughter cells retained similar epifluorescence with the parental cells (Fig. 2F1). Meanwhile, the asymmetric division was found with the strong epifluorescence on one parent cell (Fig. 2F2). After 7 days, most of the segregated cells lost epifluorescence, which indicated asymmetrical daughter cells (Fig. 2F3). However, approximately 20–30% of the cells retained higher epifluorescence in single, cell-originated tumor spheres, which indicated tumor-initiating cells with low proliferation ability (Fig. 2F3). But most SGC7901 divided symmetrically in PKH-26 assay (data not show).

The aforementioned observation indicated us CSLCs remained self-renewal ability; however, the PKH-26 is not the most accurate way to look at symmetric or asymmetric division over multiple cells divisions. Therefore, single cell were cultured with BrdU to label template DNA for 3–4 passages. More than 98% of staining cells were labeled successfully, which were counted by laser scanning confocal microscopy. Most of SGC7901 remained similar BrdU- or EDU-labeled DNA during cell division (Fig. 2G1,G2). Only 2 of 245 cells (8‰) exclusively segregated BrdU-labeled DNA template to one side of mitosis cells. And only 3 of 271 cells (11‰) inherited EDU-labeled template DNA to one side (Fig. 2G3). During mitosis, CLSCs exhibited asymmetric (Fig. 2H1) or symmetric division (Fig. 2H2) by labeling EDU or BrdU. Twenty-five percent cells (81/325) was found asymmetric segregation with one side heavily EDU-labeled DNA. Intestinally, two asymmetric divisions were observed: one inherited more template DNA to asymmetric nucleus (Fig. 2H3), and another segregated itself with two symmetric nucleus (Fig. 2H4).

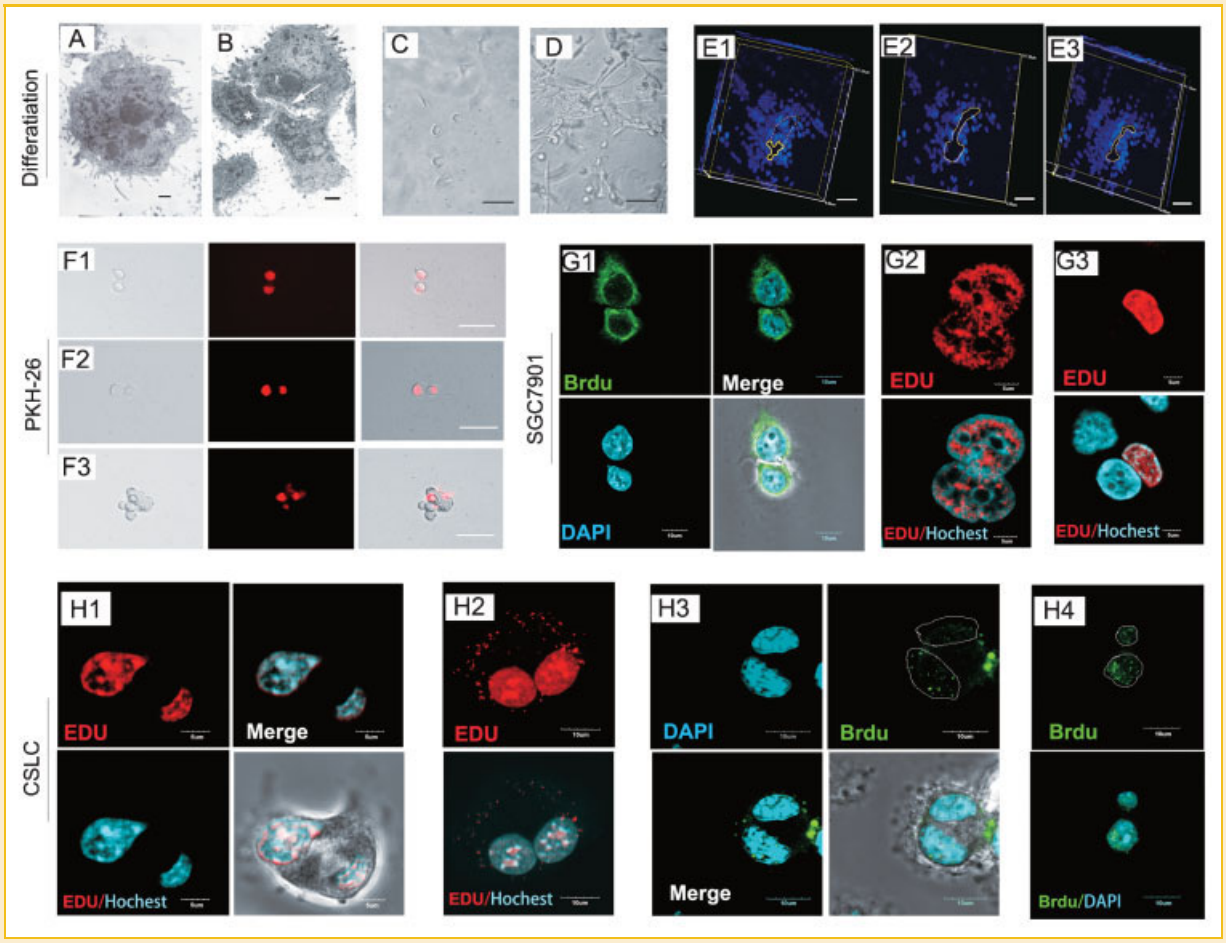

Fig. 2. CSLCs displayed differentiation ability and self-renewal ability in vitro. (A) SGC7901 cells (B) CSLCs: small primary stem cells (asterisk) with two differentiated daughter cells formed gland-like structures with microvilli (arrow) (scale bar, 1 μm). CSLCs (D) showed obvious vessel-like structure formation in 2-D than SGC7901 (C) (scale bar, 100 μm). Complex lumen-like structures examined by DAPI in 3-D (E1, E2, and E3, scale bar, 60 μm). Symmetric (F1) and asymmetric division of CLSCs (F2) were check by the remained amount of PKH-26 (red) on the first day. F3: There was about 30% asymmetric division left on the 7 day (scale bar, 200 μm). SGC7901 cells symmetric (G1,G2) or asymmetric segregation (G3) assessed by BrdU and EDU by labeling the Template of DNA. CSLCs exhibited two processes of asymmetric segregation, with one small nuclear daughter cell (H1,H4) or equal nuclear (H3). Symmetric division was also observed in CSLCs (H2).

Obvious asymmetric ability of CSLCs was observed when comparing with its parent cell line SGC7901 (25% vs. 8–11‰, $P < 0.05$, paired Student's *t*-test). Moreover, the results supported the hypothesis that the self-renewal of CSLCs significantly influenced by asymmetric division, which could be directly observed and measured in vitro.

CSLCs EXHIBITED REMARKABLE CLONE FORMATION AND TUMORIGENICITY IN VIVO

With serum stimulation, CSLCs showed higher clone formation ability than SGC7901 (Fig. 3A), and significantly increased rate of clone efficiency (Fig. 3B, $P < 0.05$). Tumorigenicity in vivo was assessed by inoculating CSLCs or their parental cells subcutaneously into nude mice. These studies revealed that CSLCs (Fig. 3F), unlike parental cells (Fig. 3E), formed measurable tumor masses in animals after 4 weeks. The growth volume was monitored every 4 days up to 8 weeks. In the experiment, CSLCs generated tumors of greater volume (Fig. 3E) and weight (Fig. 3F). The mean weight of tumors mass increased by 2.8-fold ($P < 0.05$) compared with SGC7901.

Histology H&E staining is shown in Figure 3G,H. As can be seen, the CSLCs (Fig. 3H) displayed a significant heterogeneity, with more numerous, smaller tumor cells and more abundant cytoplasm than in the parental cells (Fig. 3G). This heterogeneity indicated that small gastric CSLCs might give rise to daughter cells of different clones.

CSLCs OBTAINED MDR AND EXPRESSED SURFACE MARKERS SPECIFIC TO CSCs

Oct4 and SOX2 have been proven to be critical transcription factors in inducing pluripotency [Yamanaka, 2008; Kim et al., 2009]. Oct4A also regulates embryonic stem cells and the self-renewal and pluripotency of prostate cancer subpopulations [Lee et al., 2006; Sotomayor et al., 2009]. We therefore investigated co-expression of the embryonic proteins OCT4A, SOX2, and OCT4 by immunofluorescence in CSLCs (Fig. 4A). Interestingly, OCT-4 and its isoform OCT-4A were located in the nucleus of CSLCs. In addition, the expression of SOX2 was greatly enhanced in CSCLs compared to controls. Real-time PCR also showed the pluripotent genes SOX2, OCT4, and Musashi-1(an RNA-binding protein) regulated by the

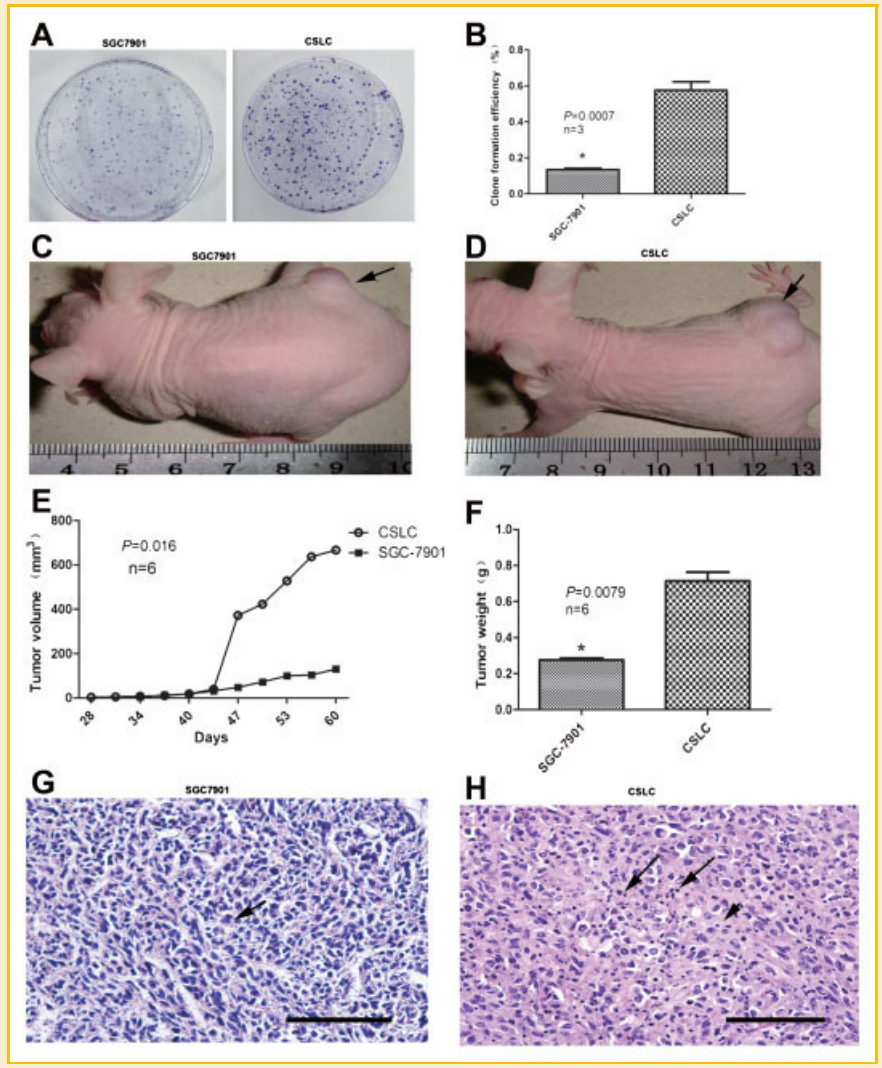

Fig. 3. Remarkable clone formation and tumorigenicity with CSLCs in vivo and vitro. CSLC proliferated faster than SGC7901 assessed by plate clone (A,B). Clone formation efficiency was analyzed (C). CSLC (1×10^5 cells) were subcutaneously inoculated into nude mice. CSLCs produced much larger tumors than VCR-induced SGC7901 cells after 8 weeks (C,D). Tumor growth was measured every 4 days and significant tumor mass was found in CSLC group (E,F). Histology revealed heterogeneity in the sections of subcutaneous tumors derived from CSLC compared to SGC7901 control (G,H) (arrow, heterogeneity in nuclei; arrow head, the cytoplasm and mucous) (scale bar, 200 μm, asterisk, paired Student's *t*-test).

canonical Wnt pathway and proposed as a marker of intestinal epithelial stem cells [Rezza et al., 2010] were up-regulated in CSLCs (Fig. 4B).

The resistance of VCR-induced CSLCs and parental cells to ADR, VCR, epitubincin (EPI), and 5-FU was determined. The sensitivity and cell viability were valued by IC_{50} according to a previous study [Zhao et al., 2009]. The MTT assay revealed that VCR-induced CSLCs exhibited greatly enhanced drug resistance to VCR, ADR, EPI, and 5-FU compared to parental cells, as indicated by significantly increased IC_{50} values. The mean increases in IC_{50} values were approximately 8- to 20-fold in the CSLCs (Fig. 4C). The red fluorescence intensity of EPI was detected by fluorescent microscopy also showed more than 90% of the CSLCs survived by the efflux of EPI, significant higher than SGC7901 [Zhao et al., 2009] (excitation 488 nm and emission 575 nm; data not show).

To identify gastric CSC markers, which are helpful for sorting and studying subpopulations, we examined the expression of CD44, CD90, CD133, EpCAM, CXCR4, Bmi-1, and musashi-1 by real-time PCR. As can be seen, CD44, CD90, and CXCR4 were more highly expressed in the VCR-induced CSLCs than in the SGC7901 parental cells (Fig. 4B). The other lumen-like genes, SOX2 and CDX2 [Lorentz et al., 1997; Qualtrough et al., 2002], were also significantly up-regulated in the VCR-induced CSLCs (Fig. 4B). CSLCs surface marker CD44 was explored by FACS. We found that there were 99% positive cells with SGC7901 (Fig. 4D), but these cells did not show significant tumor sphere clone ability. VCR preconditioned SGC7901 with 24 h also exhibited 99% CD44 positive (Fig. 4E). However, the more aggressive CSLCs showed low expression of CD44 (83.5%, Fig. 4F), which indicated us the different CD44 expression in gene level and protein level.

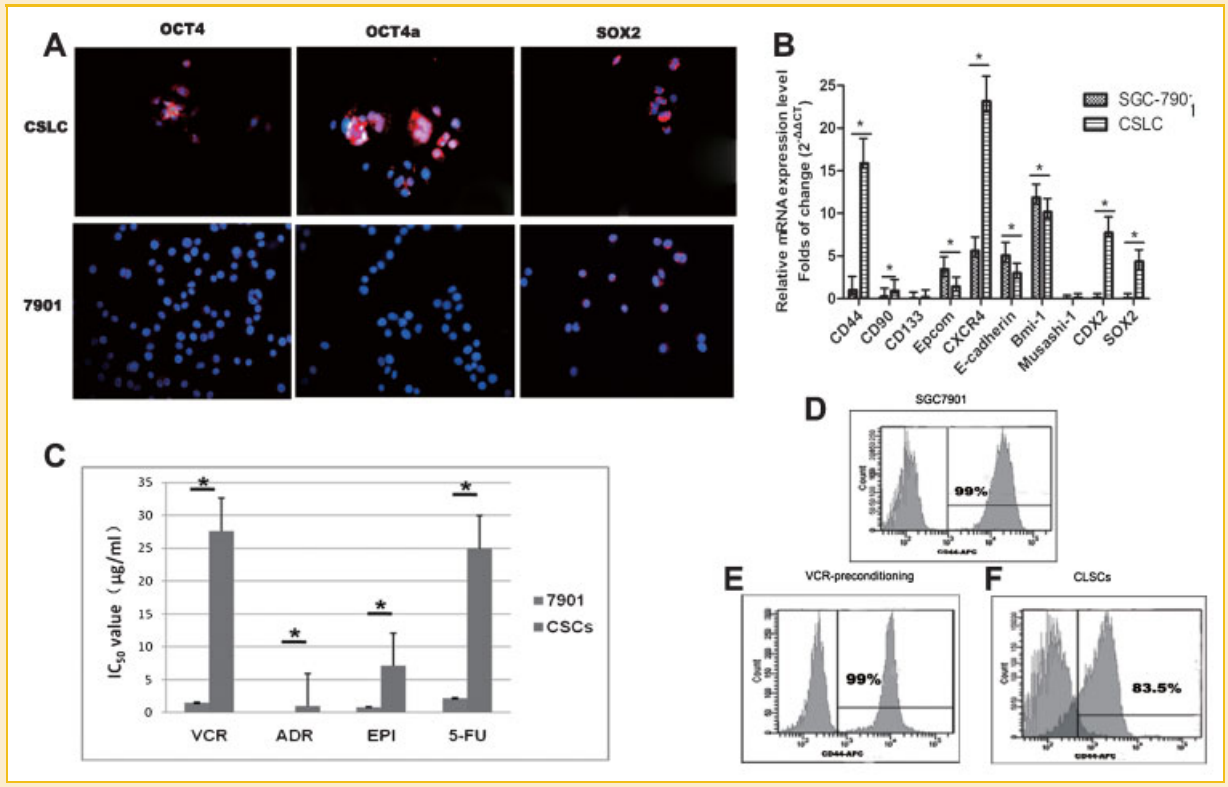

Fig. 4. MDR and stem cell surface markers were examined in CSLCs. A: CSLCs showed up-regulation of OCT4, OCT4a, and SOX2 (red) compared to SGC7901 cells. Nuclei were stained by DAPI (blue). B: Different stem cell markers were screened in VCR-induced CSLCs by real-time PCR. C: Cell viability was assessed using the MTT assay, and IC_{50} values for each drug were compared between VCR-induced CSLCs and SGC7901. The data are the mean ± SD from three independent experiments. D,E: CD44 was found 99% positive in SGC7901 and VCR-preconditioning 24 h SGC7901. CSLCs accounted for only 83.5% CD44 (+) cells (scale bar, 200 μm; asterisk, $P < 0.05$, paired Student's *t*-test).

DISCUSSION

We report here a transient preconditioning method using VCR to enrich gastric CSLCs in vitro. The self-renewal and differentiation abilities of these VCR-induced CSLCs were then demonstrated in vitro. Our CSC models determined the existence of CSCs in induced cells, which accounted for MDR and recurrence in solid tumors [Dean et al., 2005; Kurrey et al., 2009]. Most CSC assays enrich CSCs from primary tumor tissue using FACS sorting, which depends on cell-surface markers [Visvader and Lindeman, 2008; Yeung et al., 2010]. Such sorting assays are considered to be cumbersome, expensive and difficult for the study of functional characteristics [Yeung et al., 2010]. Furthermore, cell lines represent a valuable resource for the induction of CSCs or CSLCs for study because the cells can be reused and are easily scaled up in vitro, unlike primary human cancer tissues [Takaishi et al., 2009].

There is strong evidence that cell lines can represent their original, isolated tumors [Douglas et al., 2004] and develop structures similar to those original tissues [Yeung et al., 2010]. Thus, in the present study, the goal was to prove that CSCs or CSLCs could be induced and verified in gastric cancer-derived cells. VCR-preconditioned method significantly improved the proportion of tumor sphere formation from 5% to 25% in vitro. Yu et al. [2008] have also evaluated VCR function for isolating CSCs from a human glioblastoma cell line and have found that VCR could effectively increase the ability of tumor sphere formation. As a mitotic inhibitor, the mechanism of how VCR regulates the capacity of sphere formation is still unknown, but the inhibiting of microtubule structures and disruption of the mitosis might induce CSCs formation. In addition, our results indicated that VCR mediated EMT and dedifferentiation benefited CSC formation efficiency. VCR mediated the up-regulation of the critical EMT genes Snail and Twist. Snail and Twist are core transcription factors and play major roles in EMT and dedifferentiation [Weinberg, 2008; Taube et al., 2010]. Previous studies have also shown overexpression of Twist by ADR and paclitaxel treatment, which caused breast cancer cells to acquire mesenchymal-like phenotypes and MDR and to resist apoptosis and promote invasion [Cheng et al., 2007; Li et al., 2009]. The up-regulation of Twist and Snail in CSLCs upon transient VCR treatment was also found in our study, which indicates the activation of mesenchymal genes and the enrichment of CSLCs after VCR treatment. This conclusion was further confirmed by the down-regulation of the epithelial marker protein E-cadherin and up-regulation of the mesenchymal marker vimentin.

CD44, which was identified from the gastric cell lines AGS, MKN28, and KATO-III, is recognized as a candidate surface marker of gastric CSCs [Takaishi et al., 2009]. However, the higher percentage of CD44-positive cells hinders gastric studies [Takaishi et al., 2009]. In this report, gastric cancer cell line SGC7901 showed CD44 was 99% positive, but these cells exhibited lower tumor sphere

efficiency and oncogenic capability than CLSCs. Therefore, CXCR4 or CD90 might be the candidate marks and CD44 cannot be supposed to one accurate surface marker, Recent study has found CD90 is a gastric CSCs marker [Jiang et al., 2011]. EpCAM(+)/CD44(+) have been reported in gastric stem cells [Han et al., 2011], but EpCAM down-regulated in our study. Interestingly, CLSCs were also isolated from SGC7901 cell line with different method [Yang et al., 2011].

CSCs share similar characteristics with tissue stem cells, including differentiation and self-renewal [Eyler and Rich, 2008; Gupta et al., 2009a]. However, there are no well-developed approaches to enrich CSCs or CSLCs for investigating the properties of differentiation and self-renewal in gastric CSCs in vitro. Hence, we developed a new approach to obtain VCR-preconditioning CSLCs. We observed an unanticipated phenomenon using transmission electron microscopy wherein one primary CSLC with two daughter cells formed gland-like structures with microvilli. This observation indicated that the subpopulation of tumor spheres possessed differentiation ability, even in serum-free media. Subsequently, gastric CSLCs formed vessel-like and lumen-like complex structures in 2-D and 3-D Matrigel cultures, as seen under a confocal microscope.

Using a Matrigel-based differentiation assay, colon CSCs differentiated into complex, 3-D structures that were considered to be direct evidence of the existence of CSCs from the colon cancer cell line SW1222 [Yeung et al., 2010]. Unfortunately, there is a lack of specific differentiation markers to label differentiated cells of gastric CSCs. Accordingly, we used the gastric differentiation markers CDX2 [Lorentz et al., 1997; Qualtrough et al., 2002; Barker et al., 2010] and SOX2 [Tatematsu et al., 2003; Tsukamoto et al., 2004; Park et al., 2008] to validate these gland-like structures. Tatematsu et al. [2003] reported that the ectopic expression of CDX2 and SOX2 in normal gastric stem cells implied intestinal and gastric differentiation direction. In our study, we found that CDX2 and SOX2 were significantly up-regulated in CSLCs. Furthermore, computational modeling of the 3-D gland reconstruction provided strong evidence for gland differentiation under confocal microscope examination. However, differentiation markers need to be further investigated in VCR-induced CSLCs.

Self-renewal is one of the characteristics of gastric CSCs, but direct evidence is still lacking, mainly due to a poor understanding of the biological differences between normal and CSCs [Cicalese et al., 2009]. Asymmetric division is a recognizable characteristic of stem cells that retain self-renewal and generate differentiated progeny [Morrison and Kimble, 2006]. However, stem cells also possess the ability to expand in number by symmetric division, which occurs during development or after injury [Morrison and Kimble, 2006; Cicalese et al., 2009]. Moreover, asymmetric division was also found in lung cancer cell and primary tumor cells from patients [Pine et al., 2010], we also observed the asymmetric division of SGC7901 with the rate of 8–11‰, which was significant lower than CLSCs.

Symmetric and asymmetric divisions are considered to be key adaptations and responses to a niche [Pine et al., 2010]. PKH-26, BrdU, and EDU which label relatively quiescent cells with membrane and the template of DNA separately, are able to differentiate symmetric from asymmetric division [Pece et al., 2010; Pine et al., 2010]. Symmetric division is identified by fluorescence intensity or the template of DNA. In the current study, we noticed that there were both symmetric and asymmetric divisions in VCR-induced CSLCs. Specifically, 20–30% of CSLCs retained asymmetric by tracing 7–14 days. A possible reason for this is that the SGC7901 cell line is derived from a low-differentiation gastric adenocarcinoma with a P53 mutation [Jiang et al., 2001]. These P53-mutant stem cells self-renew, with unlimited and symmetric division, more frequently than their normal counterparts [Cicalese et al., 2009]. CSLCs with high tumorigenicity were demonstrated by xenograft study. CSLCs H&E staining displayed a significant heterogeneity, which indicated that small gastric CSLCs might give rise to daughter cells in vivo. However, no significant gland was found.

Of note, we demonstrated the existence of gastric CSLCs by transient VCR treatment in vitro. Additionally, we established a set of assays to study the self-renewal and differentiation abilities of CSLCs. This is the first time that both asymmetric and symmetric division have been observed to exist in gastric CSLCs induced by VCR treatment from P53-mutant gastric cancer cells.

ACKNOWLEDGMENTS

We thank Yongquan Shi for constructive advice. This study was supported by the National Basic Research Program of China (No. 2010CB529300, No. 2010CB529306 and 2010CB529302) and the National Natural Science Foundation of China (No.81030044 and No. 30871143).

REFERENCES

Ansieau S, Bastid J, Doreau A, Morel AP, Bouchet BP, Thomas C, Fauvet F, Puisieux I, Doglioni C, Piccinin S, Maestro R, Voeltzel T, Selmi A, Valsesia-Wittmann S, Caron de Fromentel C, Puisieux A. 2008. Induction of EMT by twist proteins as a collateral effect of tumor-promoting inactivation of premature senescence. Cancer Cell 14:79–89.

Arumugam T, Ramachandran V, Fournier KF, Wang H, Marquis L, Abbruzzese JL, Gallick GE, Logsdon CD, McConkey DJ, Choi W. 2009. Epithelial to mesenchymal transition contributes to drug resistance in pancreatic cancer. Cancer Res 69:5820–5828.

Barker N, Huch M, Kujala P, van de Wetering M, Snippert HJ, van Es JH, Sato T, Stange DE, Begthel H, van den Born M, Danenberg E, van den Brink S, Korving J, Abo A, Peters PJ, Wright N, Poulsom R, Clevers H. 2010. Lgr5(+ve) stem cells drive self-renewal in the stomach and build long-lived gastric units in vitro. Cell Stem Cell 6:25–36.

Bjerkvig R, Tysnes BB, Aboody KS, Najbauer J, Terzis AJ. 2005. Opinion: The origin of the cancer stem cell: Current controversies and new insights. Nat Rev Cancer 5:899–904.

Cheng GZ, Chan J, Wang Q, Zhang W, Sun CD, Wang LH. 2007. Twist transcriptionally up-regulates AKT2 in breast cancer cells leading to increased migration, invasion, and resistance to paclitaxel. Cancer Res 67: 1979–1987.

Cicalese A, Bonizzi G, Pasi CE, Faretta M, Ronzoni S, Giulini B, Brisken C, Minucci S, Di Fiore PP, Pelicci PG. 2009. The tumor suppressor p53 regulates polarity of self-renewing divisions in mammary stem cells. Cell 138:1083–1095.

Dean M, Fojo T, Bates S. 2005. Tumour stem cells and drug resistance. Nat Rev Cancer 5:275–284.

Debnath J, Muthuswamy SK, Brugge JS. 2003. Morphogenesis and oncogenesis of MCF-10A mammary epithelial acini grown in three-dimensional basement membrane cultures. Methods 30:256–268.

Dontu G, Abdallah WM, Foley JM, Jackson KW, Clarke MF, Kawamura MJ, Wicha MS. 2003. In vitro propagation and transcriptional profiling of human mammary stem/progenitor cells. Genes Dev 17:1253–1270.

Douglas EJ, Fiegler H, Rowan A, Halford S, Bicknell DC, Bodmer W, Tomlinson IP, Carter NP. 2004. Array comparative genomic hybridization analysis of colorectal cancer cell lines and primary carcinomas. Cancer Res 64:4817–4825.

Eyler CE, Rich JN. 2008. Survival of the fittest: Cancer stem cells in therapeutic resistance and angiogenesis. J Clin Oncol 26:2839–2845.

Fisher HW, Cooper TW. 1967. Electron microscope studies of the microvilli of HeLa cells. J Cell Biol 34:569–576.

Gupta PB, Chaffer CL, Weinberg RA. 2009a. Cancer stem cells: Mirage or reality? Nat Med 15:1010–1012.

Gupta PB, Onder TT, Jiang G, Tao K, Kuperwasser C, Weinberg RA, Lander ES. 2009b. Identification of selective inhibitors of cancer stem cells by high-throughput screening. Cell 138:645–659.

Han ME, Jeon TY, Hwang SH, Lee YS, Kim HJ, Shim HE, Yoon S, Baek SY, Kim BS, Kang CD, Oh SO. 2011. Cancer spheres from gastric cancer patients provide an ideal model system for cancer stem cell research. Cell Mol Life Sci [Epub ahead of print].

Jiang XH, Wong BC, Lin MC, Zhu GH, Kung HF, Jiang SH, Yang D, Lam SK. 2001. Functional p53 is required for triptolide-induced apoptosis and AP-1 and nuclear factor-kappaB activation in gastric cancer cells. Oncogene 20: 8009–8018.

Jiang J, Zhang Y, Chuai S, Wang Z, Zheng D, Xu F, Li C, Liang Y, Chen Z. 2011. Trastuzumab (herceptin) targets gastric cancer stem cells characterized by CD90 phenotype. Oncogene [Epub ahead of print].

Kalluri R, Weinberg RA. 2009. The basics of epithelial-mesenchymal transition. J Clin Invest 119:1420–1428.

Kim JB, Sebastiano V, Wu G, Arauzo-Bravo MJ, Sasse P, Gentile L, Ko K, Ruau D, Ehrich M, van den Boom D, Meyer J, Hubner K, Bernemann C, Ortmeier C, Zenke M, Fleischmann BK, Zaehres H, Scholer HR. 2009. Oct4-induced pluripotency in adult neural stem cells. Cell 136:411–419.

Kurrey NK, Jalgaonkar SP, Joglekar AV, Ghanate AD, Chaskar PD, Doiphode RY, Bapat SA. 2009. Snail and slug mediate radioresistance and chemoresistance by antagonizing p53-mediated apoptosis and acquiring a stem-like phenotype in ovarian cancer cells. Stem Cells 27:2059–2068.

Lee J, Kim HK, Rho JY, Han YM, Kim J. 2006. The human OCT-4 isoforms differ in their ability to confer self-renewal. J Biol Chem 281:33554–33565.

Li Q-Q, Xu J-D, Wang W-J, Cao X-X, Chen Q, Tang F, Chen Z-Q, Liu X-P, Xu Z-D. 2009. Twist1-mediated adriamycin-induced epithelial-mesenchymal transition relates to multidrug resistance and invasive potential in breast cancer cells. Clin Cancer Res 15:2657–2665.

Lorentz O, Duluc I, Arcangelis AD, Simon-Assmann P, Kedinger M, Freund J-N. 1997. Key role of the Cdx2 homeobox gene in extracellular matrix-mediated intestinal cell differentiation. J Cell Biol 139:1553–1565.

Mani SA, Guo W, Liao MJ, Eaton EN, Ayyanan A, Zhou AY, Brooks M, Reinhard F, Zhang CC, Shipitsin M, Campbell LL, Polyak K, Brisken C, Yang J, Weinberg RA. 2008. The epithelial-mesenchymal transition generates cells with properties of stem cells. Cell 133:704–715.

Morel AP, Lievre M, Thomas C, Hinkal G, Ansieau S, Puisieux A. 2008. Generation of breast cancer stem cells through epithelial-mesenchymal transition. PLoS ONE 3:e2888.

Morrison SJ, Kimble J. 2006. Asymmetric and symmetric stem-cell divisions in development and cancer. Nature 441:1068–1074.

Park ET, Gum JR, Kakar S, Kwon SW, Deng G, Kim YS. 2008. Aberrant expression of SOX2 upregulates MUC5AC gastric foveolar mucin in mucinous cancers of the colorectum and related lesions. Int J Cancer 122:1253–1260.

Parkin DM, Bray F, Ferlay J, Pisani P. 2005. Global cancer statistics, 2002. CA Cancer J Clin 55:74–108.

Pece S, Tosoni D, Confalonieri S, Mazzarol G, Vecchi M, Ronzoni S, Bernard L, Viale G, Pelicci PG, Di Fiore PP. 2010. Biological and molecular heterogeneity of breast cancers correlates with their cancer stem cell content. Cell 140:62–73.

Pine SR, Ryan BM, Varticovski L, Robles AI, Harris CC. 2010. Microenvironmental modulation of asymmetric cell division in human lung cancer cells. Proc Natl Acad Sci USA 107:2195–2200.

Qiao XT, Ziel JW, McKimpson W, Madison BB, Todisco A, Merchant JL, Samuelson LC, Gumucio DL. 2007. Prospective identification of a multilineage progenitor in murine stomach epithelium. Gastroenterology 133: 1989–1998.

Qualtrough D, Hinoi T, Fearon E, Paraskeva C. 2002. Expression of CDX2 in normal and neoplastic human colon tissue and during differentiation of an in vitro model system. Gut 51:184–190.

Rezza A, Skah S, Roche C, Nadjar J, Samarut J, Plateroti M. 2010. The overexpression of the putative gut stem cell marker Musashi-1 induces tumorigenesis through Wnt and Notch activation. J Cell Sci 123:3256–3265.

Rosen JM, Jordan CT. 2009. The increasing complexity of the cancer stem cell paradigm. Science 324:1670–1673.

Sathananthan AH, Nottola SA. 2007. Digital imaging of stem cells by electron microscopy. Methods Mol Biol 407:21–41.

Sotomayor P, Godoy A, Smith GJ, Huss WJ. 2009. Oct4A is expressed by a subpopulation of prostate neuroendocrine cells. Prostate 69:401–410.

Takaishi S, Okumura T, Tu S, Wang SS, Shibata W, Vigneshwaran R, Gordon SA, Shimada Y, Wang TC. 2009. Identification of gastric cancer stem cells using the cell surface marker CD44. Stem Cells 27:1006–1020.

Tatematsu M, Tsukamoto T, Inada K. 2003. Stem cells and gastric cancer: Role of gastric and intestinal mixed intestinal metaplasia. Cancer Sci 94:135–141.

Taube JH, Herschkowitz JI, Komurov K, Zhou AY, Gupta S, Yang J, Hartwell K, Onder TT, Gupta PB, Evans KW, Hollier BG, Ram PT, Lander ES, Rosen JM, Weinberg RA, Mani SA. 2010. Core epithelial-to-mesenchymal transition interactome gene-expression signature is associated with claudin-low and metaplastic breast cancer subtypes. Proc Natl Acad Sci USA 107:15449–15454.

Todaro M, Francipane MG, Medema JP, Stassi G. 2010. Colon cancer stem cells: Promise of targeted therapy. Gastroenterology 138:2151–2162.

Tsukamoto T, Inada K, Tanaka H, Mizoshita T, Mihara M, Ushijima T, Yamamura Y, Nakamura S, Tatematsu M. 2004. Down-regulation of a gastric transcription factor, Sox2, and ectopic expression of intestinal homeobox genes, Cdx1 and Cdx2: Inverse correlation during progression from gastric/intestinal-mixed to complete intestinal metaplasia. J Cancer Res Clin Oncol 130:135–145.

Visvader JE, Lindeman GJ. 2008. Cancer stem cells in solid tumours: Accumulating evidence and unresolved questions. Nat Rev Cancer 8:755–768.

Wang Z, Li Y, Kong D, Banerjee S, Ahmad A, Azmi AS, Ali S, Abbruzzese JL, Gallick GE, Sarkar FH. 2009. Acquisition of epithelial-mesenchymal transition phenotype of gemcitabine-resistant pancreatic cancer cells is linked with activation of the notch signaling pathway. Cancer Res 69: 2400–2407.

Weinberg RA. 2008. Twisted epithelial-mesenchymal transition blocks senescence. Nat Cell Biol 10:1021–1023.

Xia L, Zhang D, Du R, Pan Y, Zhao L, Sun S, Hong L, Liu J, Fan D. 2008. miR-15b and miR-16 modulate multidrug resistance by targeting BCL2 in human gastric cancer cells. Int J Cancer 123:372–379.

Yamanaka S. 2008. Induction of pluripotent stem cells from mouse fibroblasts by four transcription factors. Cell Prolif 41(Suppl 1):51–56.

Yang L, Ping YF, Yu X, Qian F, Guo ZJ, Qian C, Cui YH, Bian XW. 2011. Gastric cancer stem-like cells possess higher capability of invasion and metastasis in association with a mesenchymal transition phenotype. Cancer Lett 310:46–52.

Yeung TM, Gandhi SC, Wilding JL, Muschel R, Bodmer WF. 2010. Cancer stem cells from colorectal cancer-derived cell lines. Proc Natl Acad Sci USA 107:3722–3727.

Yu SC, Ping YF, Yi L, Zhou ZH, Chen JH, Yao XH, Gao L, Wang JM, Bian XW. 2008. Isolation and characterization of cancer stem cells from a human glioblastoma cell line U87. Cancer Lett 265:124–134.

Zeisberg M, Neilson EG. 2009. Biomarkers for epithelial-mesenchymal transitions. J Clin Invest 119:1429–1437.

Zhao L, Pan Y, Gang Y, Wang H, Jin H, Tie J, Xia L, Zhang Y, He L, Yao L, Qiao T, Li T, Liu Z, Fan D. 2009. Identification of GAS1 as an epirubicin resistance-related gene in human gastric cancer cells with a partially randomized small interfering RNA library. J Biol Chem 284:26273–26285.